

SKILL-ALIGNED FAIRNESS IN MULTI-AGENT LEARNING FOR COLLABORATION IN HEALTHCARE *

Promise Ekpo
Cornell Tech, NY, USA
poe6@cornell.edu

Brian La
Cornell Tech, NY, USA
by18@cornell.edu

Thomas Wiener
Cornell Tech, NY, USA
tfw29@cornell.edu

Saasha Agarwal
Cornell Tech, NY, USA
sa2388@cornell.edu

Arshia Agrawal
Cornell Tech, NY, USA
aa2443@cornell.edu

Gonzalo Gonzalez-Pumariega
Cornell Tech, NY, USA
gg387@cornell.edu

Lekan Molu
Microsoft Research, NY, USA
patlekano@gmail.com

Angelique Taylor
Cornell Tech, NY, USA
amt298@cornell.edu

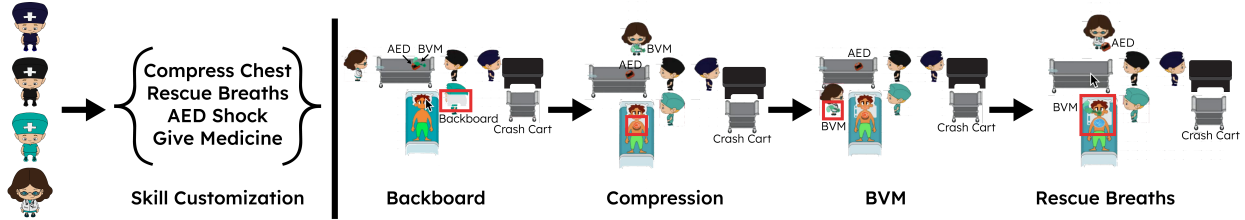


Figure 1: **MARL Hospital Environment.** The environment integrates a PDDL planner with a MARL state layer to model skill-aligned fairness and shared-task coordination among healthcare workers. The goal is to pick the backboard from the crash cart, move to the patient, place it under the patient, compress patient chest multiple times, retrieve the Bag-Valve-Mask (BVM) from the crash cart, give patient rescue breaths multiple times.

ABSTRACT

Fairness in Multi-Agent reinforcement learning (MARL) is often framed as a workload balance problem, overlooking agent expertise and the structured coordination required in real-world domains. In healthcare, equitable task allocation requires both workload balance and skill-task alignment to prevent burnout and overuse of highly skilled agents. We make two contributions to address this problem. First, we introduce MARLHospital, a customizable healthcare-inspired environment for training and evaluating team compositions and energy-constrained scheduling impacts on fairness using state-of-the-art MARL algorithms. Second, we propose FairSkillMARL, a framework that defines fairness as the dual objective of workload balance and skill-task alignment. FairSkillMARL achieves higher alignment and comparable or lower workload disparity than workload-only baselines, improving coordination by up to 60% without reducing success rates. Results show that aligning effort with expertise enables more coordinated and fair multi-agent behavior. Our work provides tools and a foundation for studying fairness in heterogeneous multi-agent systems.

Keywords Multi-agent systems · Healthcare · Fairness · Benchmark

**Citation:* Promise Osaine Ekpo, Brian La, Thomas Wiener, Saasha Agarwal, Arshia Agrawal, Gonzalo Gonzalez-Pumariega, Lekan P. Molu, Angelique Taylor. Skill-Aligned Fairness in Multi-Agent Learning for Collaboration in Healthcare. Pages.... DOI:000000/11111.

1 Introduction

In multi-agent systems, agents must learn to cooperate while leveraging resources in their environment to achieve individual and collective objectives [?]. In this paper, we are interested in effectively modeling coordination among healthcare workers (HCWs) as a multi-agent system in safety-critical environments, such as the Emergency Department (ED). A distinguishing feature of these environments that necessitates new tools to model behavior is the need for workers to perform shared tasks and occasionally relieve other workers based on availability, effort, and skills.

Common medical procedures in the ED are composed of high-level tasks and subtasks that must be carried out sequentially to achieve a goal. This includes *individual tasks* such as the use of an automated external defibrillator and administering medication, and *shared tasks* such as Cardiopulmonary resuscitation (CPR); CPR requires multiple agents to perform task-switching once they become fatigued from performing chest compressions. In real-world environments, many HCWs are overworked (i.e., burnout) when assigned tasks that do not align with their expertise (i.e., skill-task misalignment). When this happens, HCWs spend more time accomplishing tasks compared to a skilled HCW with relevant expertise who can perform the task more efficiently [1, 2, 3]. To prevent burnout and to ensure fairness in EDs, in this work, we propose a framework for fairness in a multi-agent reinforcement learning (MARL) setting.

As a first step towards a fairness framework for MARL for varying-skilled heterogeneous agents, such as in the ED, we have three requirements. First, we require a multi-agent simulation environment that captures the challenges faced by HCWs during medical procedures. Prior classes of MARL algorithms, including Independent learning (IL) [4, 5] and Centralized Training with Decentralized Execution (CTDE) algorithms [6, 7], have been benchmarked on cooperative applications where multiple agents must work together to achieve a goal; however, limited work addressed the unique challenges faced by healthcare workers in ED scenarios.

Second, simulators provide a controlled environment for modeling and analyzing cooperative tasks among multiple agents, thereby facilitating detailed optimization and evaluation of team dynamics and coordination [8, 9, 10, 11]; yet, existing simulators lack realistic healthcare-themed environments that model agents’ level of energy while taking actions, team compositions, and expertise.

Third, prior work has quantified fairness as reward equality in social dilemmas [12], worst-case performance guarantees in traffic scheduling [13], balanced throughput in network control [14, 15], equitable effort distribution in cooperative navigation tasks [16], cumulative reward parity in hierarchical learning (such as Fair-Efficient Networks, [17] and demographic parity in resource allocation [18]. However, these definitions do not jointly account for the skill-task alignment and overutilization of agents who are repeatedly tasked with the most demanding actions. Furthermore, existing simulators lack realistic healthcare-themed environments that model agent energy levels, skill-task alignment, and workload in structured team configurations. More broadly, the intersection of MARL, healthcare, and fairness is understudied.

To address these research gaps, we introduce MARLHospital, a simulation environment that captures HCWs’ interactions during medical procedures in Figure 1. MARLHospital is beneficial because it models structured teams with varying expertise, in tasks inspired by real-world medical procedures, and uniquely includes the execution of order-dependent and shared-task mode where agents alternate actions due to energy constraints, modelling agent fatigue across long time horizons, unlike prior work [8, 9, 10, 11]. Furthermore, we introduce FairSkillMARL, a framework that formulates fairness as a balance of workload and skill-task alignment during collaborative tasks, whilst factoring in the progressively dissipative energy levels of agents. This framing has the potential to improve the efficiency of healthcare teams by leveraging task-switching and agent expertise.

Our **contributions** are threefold: 1) We introduce a customizable hospital-themed game environment inspired by real-world settings. Unlike most existing MARL simulators, which target abstract coordination or traffic control, our environment models sequential, order-dependent medical procedures and structured team roles, filling a critical gap for evaluating fairness in healthcare applications. 2) We share insights about the performance of four standard MARL algorithms, including on-policy and off-policy methods, across varying team compositions, task difficulties, and energy levels in three healthcare benchmark tasks. 3) We introduce a FairSkillMARL framework, which redefines fairness as a composite disparity of agent skill-task alignment and workload, and our results demonstrate that FairSkillMARL shows competitive performance alongside state-of-the-art fairness metrics, particularly for simulated tasks and the need for more robust metrics to capture skill misalignment. We extend fairness in MARL beyond workload balance to include skill-task alignment introducing new metrics and a healthcare-inspired benchmark that enables the evaluation of cooperative policies in realistic, heterogeneous team settings.

Table 1: Comparison between *MARLHospital* and other multi-agent simulators.

	MARL	Partial-Obs.	Hospital Setting	Skill Specialization	Variable Skills	Shared Tasks
Overcooked-AI [8]	X	X	X	X	X	X
Agent Hospital [19]	X	✓	✓	X ¹	X	X
MARL Robotic Surgery [20]	✓	✓	✓ ²	✓	X	X
MARL for Nurse Rostering [21]	✓	X	✓ ³	X	X	X
Cuisine World [22]	X	X	X	X	X	X
VirtualHome [23]	X	X	X	X	X	X
SMACv2 [11]	✓	✓	X	✓	X	X
Pommerman [24]	✓	✓	X	X	X	X
Melting Pot 2.0 [25]	✓	✓	X	✓	X	X
Robotouille [9]	X	X	X	X	X	X
HMARL for Medical Allocation [26]	✓	X ⁴	X	X	X	X
MA Hospital Infection Sim [27]	X	X	✓	✓	X	X
H2-MARL [28]	✓	✓	✓	X	X	X
NurseSchedRL [29]	✓	X	✓	✓ ⁷	X	X
MedScrubCrew [30]	X	X	✓	X	X	X
Multi-Agent Collaborative Work Sim [31]	X	X	✓	✓	X	X
Hierarchical MA Resource Allocation [26]	✓	X ⁴	✓	X	X	X
Fair-PPO HospitalSim [18]	✓	X ⁵	✓	X ⁶	X	X
<i>MARLHospital (Ours)</i>	✓	✓	✓	✓	✓	✓

¹ Patients, doctors, and nurses modeled; no specialization among HCWs (doctors are the only “trained” agents).

² Simulates surgical actions in an OR; does not represent full hospital topology.

³ Focused on combinatorial scheduling; no patient treatment interactions.

⁴ Imperfect information handled via custom uncertainty; not formulated as an explicit POMDP.

⁵ Event-driven flow-based simulation of daily hospital logistics; no timestep-based POMDP structure.

⁶ Fairness across patient groups, not worker skill heterogeneity.

⁷ Uses fixed nurse skill profiles for assignment; profiles do not evolve during an episode.

2 Related Work

Multi-agent systems. Multi-agent systems model interactions between multiple agents in cooperative, competitive, and mixed settings. Our research explores two classes of multi-agent reinforcement learning (MARL) algorithms, Independent Q-Learning (IQL) [4] and Centralized Training with Decentralized Execution (CTDE) [32].

IQL agents simultaneously learn a Q-function within the same environment based solely on its local observations and actions, and *Independent Proximal Policy Optimisation* (IPPO) [5], which applies the popular Actor-Critic method PPO [33] independently to each agent using its own observations and actions. While these methods provide a straightforward and effective baseline in practice, the lack of global state information during training may lead to difficulty in learning coordination as unstable learning may stem from the problem of environment non-stationarity.

In CTDE [32], agents are trained using shared global information but learn policies conditioned only on their local observations, enabling effective cooperative behavior while maintaining individual decision-making during execution time. While some CTDE algorithms focus on factorizing the team’s joint action-value function into multiple individual action-value functions that can be used during deployment such as *Value Decomposition Networks* (VDN) [6], *QMIX* [7], both Q-based learning methods that backpropagate global gradients to local agent networks. Another category of CTDE algorithms uses centralized policy gradient methods involving individual actors and centralized critics (e.g *Multi-Agent PPO (MAPPO)* [34] and *Counterfactual Multi-Agent Policy Gradients (COMA)* [35]). More relevant to our setting, recent MARL applications in healthcare have used Hierarchical MARL to delegate task specialization effectively, [26, 36, 37], but this framework assumes centralized decision making will be possible at deployment.

Multi-agent environments. To understand interactions between multiple agents, the majority of research efforts have captured popular settings such as games [38, 8] and cooking environments [39]. Despite their successes, many approaches did not take into account the need for fully customizable skill levels across agents or the evaluation of predefined team compositions inspired by human-human collaboration in safety-critical environments. Although simulators such as Overcooked-AI [8] and Robotouille [39] model tasks with temporal dependencies, they assume symmetric agent expertise and lack support for evaluating different team compositions. SMACv2 [11] supports heterogeneous agents but does not support structured task hierarchies and the shared task mode in MARLHospital.

While Pommerman [24], CUISINEWORLD [22], and Melting Pot [25] focus on abstract coordination, they do not capture team heterogeneity or domain-specific expertise. VirtualHome [23] supports long-horizon tasks but lacks real-time multi-agent coordination, and AgentHospital [19] focuses on dialogue using Large Language Model rather than MARL benchmarking. We make a detailed comparison between MARLHospital and others in Table 1.

Fairness in multi-agent systems. Prior work has quantified fairness across multi-agent domains. In social dilemmas, inequity aversion reduces envy and guilt by penalizing outcome disparities, promoting cooperation [12]. In networked systems, fairness is often framed through worst-case guarantees, namely, maximizing the 5%-tile user data rate [13]. In traffic signal control, fairness is integrated into value functions to ensure low-traffic lanes are scheduled equally [14, 15]. These approaches focus on reward parity or throughput smoothing but assume homogeneous agents. Structural fairness has been explored in cooperative control by penalizing travel deviations to balance workload (author?) [16] and propose switching between fair and efficient subpolicies (author?) [17]. Social fairness constraints have also been encoded, such as demographic parity in Proximal Policy Optimization (PPO) [18]. While addressing various fairness goals, these works often overlook skill-agent compatibility and task-agent mismatch. In healthcare, fairness extends beyond efficiency to patient safety, requiring mechanisms that prevent HCWs fatigue from unfair workload and treatment delays caused by assigning tasks to workers outside their specialties.

Recent studies in multi-agent systems have explored many ways to define and measure fairness, such as *fair division*, *fair allocation*, and *fairness guarantees* in cooperative and learning settings. Research on *envy-freeness* has examined how to divide limited resources so that no agent prefers another agent’s share [40, 41]. Other work has focused on *resilient* and *group-based* fairness rules that ensure stable and inclusive outcomes [42, 43]. Fairness has also been studied in learning environments, such as fairness-aware reinforcement learning [44] and fairness-of-exposure in decision-making systems [45]. More recently, FAPPO [46] explored how to balance fairness and efficiency in cooperative MARL. Our **FairSkillMARL** framework builds on these directions by focusing on *skill–task alignment*, which captures how heterogeneous agents can share tasks fairly while balancing their workloads.

3 MARLHospital

We present MARLHospital, a framework for modeling multi-agent collaborative tasks in medical environments. The MARLHospital environment builds upon Robotouille [39] using the EPyMARL [47] setup for MARL algorithms. Unlike prior work, MARLHospital is a customizable multi-agent environment in terms of team compositions, shared vs. individually task modes. We draw inspiration from real-world safety-critical environments (i.e., the ED) in the design of MARLHospital where HCWs have varying skills, energy levels and workloads.

3.1 Notations and Preliminaries

We formulate MARLHospital as a decentralized partially observable Markov decision process (Dec-POMDP) [48], represented by the tuple $(I, \mathcal{S}, \mathcal{A}, T, R, \Omega, O, \gamma)$. Here $I = \{1, \dots, n\}$ denotes the set of agents; \mathcal{S} is the global state space; \mathcal{A} and Ω are the joint action and observation spaces; T is the transition kernel; R the team reward; O the observation kernel; and $\gamma \in [0, 1)$ the discount factor. \mathcal{A} and Ω are the joint action and observation spaces because the transition and observation depend on all agents acting simultaneously, the environment evolves based on their combined actions and produces observations for each of them.

Each agent $i \in I$ has a discrete local action space \mathcal{A}_i e.g. where a_i is drawn from $\mathcal{A}_i = \{1, 2, 3\}$ and an observation space Ω_i . At each timestep t , the environment is in state $\mathbf{s}_t \in \mathcal{S}$, each agent observes $\mathbf{o}_t^i \in \Omega_i$, and selects an action $\mathbf{a}_t^i \in \mathcal{A}_i$ according to its policy π^i . The team jointly executes $\mathbf{a}_t = (a_t^1, \dots, a_t^n)$ and receives the next state \mathbf{s}_{t+1} drawn from $T(\mathbf{s}_{t+1} | \mathbf{s}_t, \mathbf{a}_t)$ and a shared reward $R(\mathbf{s}_t, \mathbf{a}_t)$. Episodes terminate when all medical subtasks are complete or a time limit is reached.

The global state \mathbf{s}_t encodes all medically relevant information in a resuscitation scenario, combining symbolic, spatial, and continuous The global state includes the patient’s current state (whether chest-compressed or rescue-breathed), the locations of the three agents across six discrete stations (`hospital_cart_right`, `hospital_cart_left`, `table`, `small_hospital_cart`, `patient_legs`, `patient_bed_station`), each agent’s held item (BVM, Backboard, or patient), their discrete skill levels for chest compression and giving rescue breathes, continuous energy levels $e_{i,t} \in [0, e_{\max}]$ tracking fatigue (The subscript i,t denotes both the agent index and the timestep, which is standard in Dec-POMDP notation. It helps distinguish each agent’s energy value as it changes over time.), and binary indicators of whether CPR or rescue-breath goals have been reached. The complete state vector has 174 binary features and three continuous components. Each agent observes only a local subset \mathbf{o}_t^i containing its own position, held item, skill indicators, energy level, and partial patient information; other agents’ states remain hidden, enforcing partial observability.

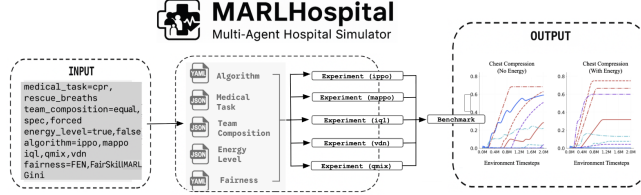


Figure 2: MARLHospital Execution flow.

Each agent’s action space \mathcal{A}_i consists of eight discrete primitives: `move`, `pick`, `place`, `stack`, `treat(patient)`, `compress_chest`, `give_rescue_breaths`, and `noop`. Actions are symbolic commands grounded in the PDDL simulator. The `compress_chest` action is an energy-constrained shared task controlled by the fatigue model in Section 3.3.1, while the remaining actions alter symbolic or spatial states without energy cost. The joint action \mathbf{a}_t therefore represents the simultaneous choices of all n agents, with $|\mathcal{A}_i| = 8$ and $|\mathcal{A}| = 8^n$ for the three-agent setting used in our experiments.

Rewards are defined through a heuristic progress function $H(\mathbf{s}_t)$ that measures advancement toward subgoals such as positioning the CPR board, picking the right items, placing the item at the right station, and completing chest compressions or administering rescue breaths. The immediate reward at timestep t is

$$R(\mathbf{s}_t, \mathbf{a}_t) = H(\mathbf{s}_t) - H(\mathbf{s}_{t-1}),$$

yielding positive values only when the team makes progress toward medical completion. Each policy π^i seeks to maximize the expected discounted return $G_t = \sum_{k=t}^T \gamma^{k-t} R(\mathbf{s}_k, \mathbf{a}_k)$.

3.2 Team Compositions

Understanding team composition is essential for modeling clinical settings, as the structure and capabilities of a care team influence task performance, decision speed, and workload distribution. We define three team compositions that vary in expertise levels (EL) of agents: *uniform*, *specialized*, and *interdependent* teams. In *uniform Teams*, all agents possess identical capabilities and can perform every subtask with equal efficiency. This structure allows maximum flexibility as any agent can complete any part of the task independently, and coordination is optional. *Specialized Teams* allows agents to be more efficient in one particular subtask but still retains the ability to perform all others, although more slowly. This specific setting incentivizes but does not necessitate collaboration. In *Interdependent Teams (Forced Cooperation)*, agents are capable of performing only a subset of subtasks and cannot execute at least two other tasks.

3.3 Medical Tasks

We model the CPR and AED tasks using the standard procedural steps of “Adult Basic Life Support” from the American Red Cross code cards in Figure 3 with the full execution flow in Figure 2. These cards provide visual flow charts guiding resuscitation procedures to capture real-world tasks based on evidence-based practices [?]. These procedural steps are modeled in the action space of MARLHospital.

3.3.1 Agent Energy Levels for Shared Tasks

Cardiopulmonary resuscitation (CPR) in real-world practice requires healthcare workers (HCWs) to alternate every two minutes to prevent fatigue [49]. To reflect this, MARLHospital introduces an **energy model** that constrains how long agents can continuously perform effort-intensive *shared tasks*, such as chest compressions (Figure 3). This mechanism enforces natural alternation between agents based on their remaining energy levels. Each agent $i \in I$ maintains an energy variable $e_{i,t}$ at timestep t , where $0 \leq e_{i,t} \leq e_{\max}$ and e_{\max} is the maximum possible energy. The initial energy levels of all agents, as well as the number of chest compressions required to reach the goal, are configurable in the simulator. Performing an action $a \in \mathcal{A}_i$ incurs an energy cost c_a : it is positive ($c_a \geq 0$) for energy-consuming actions that must be executed at maximum efficiency (e.g., `compress_chest`) and negative ($c_a < 0$) for restorative or idle actions (e.g., a “no-op” that allows recovery or any non-yellow action in Figure 3). The energy dynamics for each agent follow

$$e_{i,t+1} = \min(e_{\max}, e_{i,t} - c_a), \quad (1)$$

where c_a takes positive values for costly actions and negative values for recovery. When the simulator is in *shared-task mode*, where the energy constraint applies to the `compress_chest` action, an agent can only execute that action if it

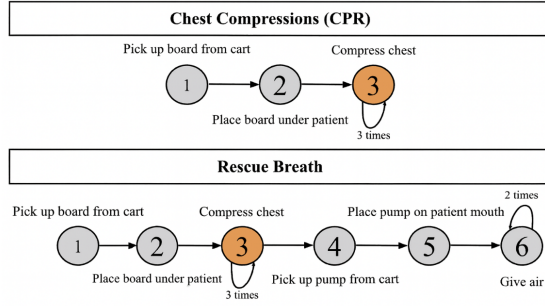


Figure 3: Task flow diagrams for the check compression (CPR) and rescue breath tasks in MARLHospital. The yellow-shaded subtask supports shared action with energy constraints.

has sufficient remaining energy:

$$a_t^i = \begin{cases} \text{compress_chest}, & \text{if } e_{i,t} \geq c_{\text{compress}}, \\ \text{noop}, & \text{otherwise.} \end{cases} \quad (2)$$

When the energy cost c_{compress} is large relative to the recharge rate $|c_{\text{noop}}|$, agents must alternate more frequently to sustain task completion. This energy model is integrated into the Dec-POMDP formulation through the state vector s_t , which includes each agent’s current energy $e_{i,t}$. By modeling fatigue directly within the state space, MARLHospital enables policies that learn both efficient task scheduling and energy-aware coordination over time.

3.3.2 Task Difficulty

We define the two goals as Partial (P) and Complete (C) with task difficulties based on the length of the time horizon. For the CPR goal, the HCWs must perform CPR, a short-time-horizon task that consists of picking up and placing a board under the patient and giving N chest compressions. For the rescue breaths, which is a longer horizon task, in addition to the CPR goal, the HCWs must perform the same actions in the CPR task, in addition to picking up and placing it on the patient to give them oxygen. Since we use procedural generation in the environment implementation, these goals can be modified in the environment configuration file.

4 FairSkillMARL

We introduce FairSkillMARL, a novel reward function that encourages agents to strike a balance between workload and skill-task alignment. Unlike prior fairness definitions that primarily focus on the distribution of agent workloads (**author?**) [16] and throughput parity [18]), in FairSkillMARL, agents are penalized for the disparity between agent workloads and the alignment between an agents’ task and expertise. A skilled agent completes complex tasks quickly with low error probability, while an unskilled agent requires more time and makes more mistakes on the same task. Our reward formulation prevents skilled agents from being overloaded with all complex tasks (causing fatigue) while also preventing unskilled agents from becoming bottlenecks on tasks beyond their capabilities. This captures the essential coordination challenge in ED, where performance depends on matching tasks to appropriate skill levels.

FairSkillMARL Objective Definition

Building on the notation introduced in Section 3.1, we now formalize the fairness objective that operates over the same agent and action spaces defined in the Dec-POMDP. We define **FairSkillMARL** as a fairness-aware objective that jointly accounts for (1) workload balance across agents and (2) alignment between an agent’s skills and the tasks it performs. Let $I = \{1, \dots, n\}$ denote the set of agents and \mathcal{T} the set of all subtasks completed in an episode. Each subtask $t \in \mathcal{T}$ is executed by one agent $i_t \in I$. Unless otherwise specified, indices $i, j \in I$ denote *agents*, while i_t refers specifically to the agent that executed subtask t .

Workload imbalance (L_1). We measure workload disparity among agents using the Gini index, which quantifies the deviation in the number of subtasks handled by each agent. Let $x_i = |\tau_i|$ denote the number of subtasks performed by

agent i , and $\bar{x} = \frac{1}{n} \sum_{i=1}^n x_i$ the mean workload across all n agents. Here i and j are agent indices used for pairwise comparisons only and can not be equal. The workload imbalance is defined as:

$$L_1 = \frac{\sum_{i=1}^n \sum_{j=1}^n |x_i - x_j|}{2n^2 \bar{x}}. \quad (3)$$

Equivalently, omitting self-pairs, $L_1 = \frac{\sum_{1 \leq i < j \leq n} |x_i - x_j|}{n(n-1)\bar{x}}$. $L_1 \in [0, 1]$ where $L_1 = 0$ represents perfectly equal workload distribution, and higher values indicate increasing inequality in the number of tasks completed by each agent.

Skill-Task Misalignment (L_2). We define L_2 as a measure of how far the team’s actual task assignments deviate from the optimal skill-to-task allocation achievable under perfect specialization. Let \mathcal{T} denote the set of all subtasks completed during an episode, and $I = \{1, 2, \dots, n\}$ the set of agents. Each subtask $t \in \mathcal{T}$ is executed by one agent $i_t \in I$, where i_t indexes the *executor* of that subtask. For comparison, we let $j \in I$ index all *candidate agents* who could have performed the same subtask. We introduce a skill function $\mathcal{S}_j(t) \in [0, 1]$ that represents the normalized proficiency or capability of agent j on task t , where higher values indicate greater expertise. The best achievable proficiency for task t across the team is therefore $\max_{j \in I} \mathcal{S}_j(t)$. Formally, we define:

$$L_2 = 1 - \frac{\sum_{t \in \mathcal{T}} \mathcal{S}_{i_t}(t)}{\sum_{t \in \mathcal{T}} \max_{j \in I} \mathcal{S}_j(t)}. \quad (4)$$

Here, i_t and j serve distinct roles: i_t refers to the agent that actually executed task t , while j ranges over all agents to determine the ideal benchmark skill for that task. The numerator measures the cumulative skill of the agents who performed each task, while the denominator measures the best possible cumulative skill if each task were assigned to its most capable agent. A lower L_2 value indicates better skill–task alignment, with $L_2 = 0$ corresponding to perfect alignment (every task performed by the most skilled agent) and $L_2 = 1$ indicating complete misalignment (no tasks aligned with agent expertise).

Composite disparity (L_3). To capture both workload balance and skill alignment, we define a composite fairness objective as a convex combination:

$$L_3 = \alpha L_1 + (1 - \alpha) L_2, \quad (5)$$

where $\alpha \in [0, 1]$ controls the trade-off between workload balance (L_1) and skill–task alignment (L_2). A higher α emphasizes equal task sharing, while a lower α prioritizes specialization consistent with agents’ expertise.

Fairness-shaped reward. Let $R : \mathcal{S} \times \mathcal{A} \rightarrow \mathbb{R}$ denote the base team reward function, and let $\lambda > 0$ control the strength of fairness regularization. The overall fairness-shaped reward used during training is:

$$r_t = R(\mathbf{s}_t, \mathbf{a}_t) - \lambda L_3, \quad (6)$$

where $\mathbf{s}_t \in \mathcal{S}$ and $\mathbf{a}_t \in \mathcal{A}$ represent the joint state and joint action at timestep t . For decentralized methods, a per-agent shaped signal $r_t^i = R_i(\mathbf{s}_t) - \lambda L_3$ can also be used, where $R(\mathbf{s}_t, \mathbf{a}_t) = \sum_i R_i(\mathbf{s}_t)$. This formulation allows FairSkillMARL to flexibly integrate fairness regularization into both Independent Learning (IL) and Centralized Training with Decentralized Execution (CTDE) algorithms, encouraging policies that are both efficient and skill-aware.

5 Experiment 1: MARLHospital

Our experiments were designed to answer the following questions: (1) How do varying task difficulty and different team compositions affect the performance of existing MARL algorithms and team efficiency? (2) How well do standard MARL algorithms perform in the shared task mode with varying energy levels, and how does this performance vary across team compositions?

5.1 Baseline Methods

Our experiments include standard MARL algorithms, including IL and CTDE, trainable on our custom simulation environment as building blocks for more sophisticated algorithms (i.e., EPyMARL library [47]² and PyMARL [10]³)

²<https://github.com/uo-epymarl>

³<https://github.com/oxwhirl/pymarl>

[50, 51, 52, 32]. We investigate structured team compositions, including standard baselines that might facilitate different coordination strategies based on their decentralized and centralized training setups.

We summarize the IL and CTDE algorithms below.

- **IQL** [4] enables each IL agent to simultaneously learn its Q-function within the environment based on its local observation history and actions.
- **MAPPO** [34] is a CTDE policy gradient algorithm. Based on the PPO framework, thus enabling multiple updates on the same training batch to improve sample efficiency and stability, but it also uses a centralised state-value critic function conditioned on the state of the global environment.
- **VDN** [6] decomposes the CTDE team’s joint Q-value function into a sum of individual Q-value functions. The joint Q-value is trained using the Deep Q-Network (DQN) algorithm [53], and thus gradients are backpropagated to the individual agent networks.
- **QMIX** [7] extends CTDE VDN by using a mixing network to combine individual agent Q-values non-linearly, allowing for more complex value function factorization. The mixing network is constrained to maintain monotonicity in the relationship between the agent-specific and global Q-values, ensuring the optimal local actions and corresponding global joint actions are the same.

5.2 Training and Testing Procedure

We benchmark state-of-the-art IL and CTDE MARL algorithms in MARLHospital with three agents. We performed task-specific hyperparameter tuning across four algorithms (see Supplemental Materials). We trained the baseline algorithms with four seeds for 50 timesteps per episode using off-policy algorithms for 2M timesteps and on-policy algorithms for 20M timesteps, similar to EPyMARL [47]. We trained off-policy algorithms using an experience replay buffer for stabilized policy learning on one NVIDIA GPU with x86 CPUs when available; otherwise, we used 4 CPU cores on a compute system with two Intel Xeon Gold 6448Y processors (each with 32 cores, 2.10–4.10GHz, 60MB cache, PCIe 5.0), providing a total of 64 CPU cores.

5.3 Measures

We use **success rate** as a performance metric to assess how often agents reach the goal. This metric allows us to understand the stability and final performance of the trained policy across all evaluation episodes. Concretely, we report the total number of goals reached out of all test episodes during test time over 4 seeds, with each evaluation consisting of 100 episodes.

5.4 Experimental Setup

We explore the impact of task difficulty, team compositions, and agent energy levels on the success rate of agents as follows:

- **Task difficulty:** To understand the impact of task difficulty, the agents perform CPR, a short time horizon task and rescue breaths, a long time horizon task.
- **Team compositions:** To assess the effect of different team compositions, the agents skills are configured as uniform, specialized, and forced cooperation.
- **Agent energy levels:** To explore the benefits of agent energy levels in the MARLHospital environment, we explore the performance of agents with and without energy function to model routine task-switching during CPR in the shared task mode.

5.5 MARLHospital Results

5.5.1 Impact of Task Difficulty on Performance.

The results in Table 2 with test success rates show that the CTDE algorithm (VDN) outperforms the DTDE algorithms in the CPR goal by a significant gap as seen in Figure 4. Additionally, in the rescue breaths goal, the CTDE (VDN, QMIX) algorithms outperform the DTDE algorithms. This indicates that CTDE approaches are more robust under increased task complexity. Also, we performed pairwise Welch’s t -tests on success rates for the chest compression task. **VDN significantly outperformed MAPPO** ($p = 0.0052$), highlighting the advantage of CTDE. Other comparisons, such as MAPPO vs. QMIX showed no significant difference.

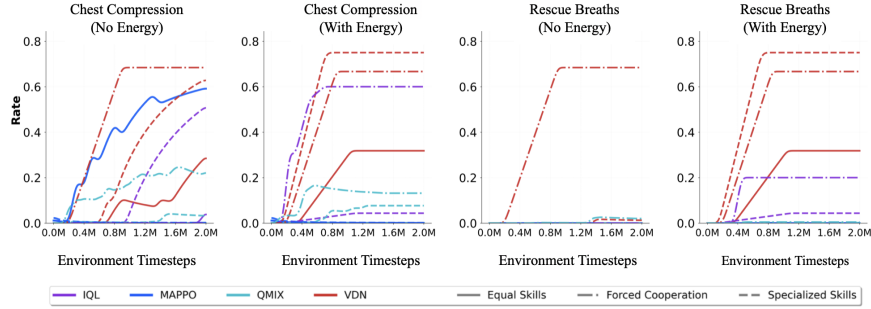


Figure 4: Test cumulative rates for the “chest compression” and “rescue breaths” tasks, with and without energy.

Table 2: Success rates of MARL algorithms for CPR (P) at energy levels 0 and 3, and Rescue Breaths (C) at energy 0, with uniform (U), specialized (S), and forced cooperation (F) team compositions (higher is better).

Method	Chest Compressions (Energy = 0)			Rescue Breaths (Energy = 0)			Chest Compressions (Energy = 3)		
	P-U	P-S	P-F	C-U	C-S	C-F	P-U	P-S	P-F
IQL [4]	0.64	0.21	0.51	0.46	0.00	0.32	0.62	0.80	0.58
MAPPO [34]	0.15	0.02	0.02	0.01	0.01	0.00	0.70	0.97	0.57
VDN [6]	0.85	0.79	0.70	0.80	0.74	0.61	0.84	0.78	0.85
QMIX [7]	0.84	0.68	0.54	0.78	0.60	0.40	0.79	0.60	0.63

5.5.2 Impact of Team Composition on Performance.

Using the same test success rates metric, the results show that CTDE specifically, VDN consistently outperformed DTDE methods across team compositions, indicating strong generalizability to different team dynamics (see Table 2). VDN has the highest success rate in the uniform skilled teams in both tasks. However, the forced cooperation teams had the lowest success rates across all algorithms, reflecting the coordination burden imposed by asymmetric skill levels of agents. This performance drop highlights the challenge of learning robust policies when agents are unable to act interchangeably.

5.5.3 Impact of Energy Function on Performance.

For the CPR goal, according to Table 2, the shared task mode (with an energy cost of “3” and recharge rate of “1”) impacts the MARL algorithm’s performance compared to the baseline scenario (energy cost of “0”). Under this setting, coordination becomes more challenging, as agents must alternate actions and manage limited energy budgets across a long-horizon task. Despite this, the CTDE algorithm VDN shows the best performance in both the uniform (PUE = 0.84) and forced cooperation (PFE = 0.85) teams, outperforming all DTDE baselines. This suggests that centralized training may help agents better learn coordination strategies under resource constraints. In contrast, DTDE methods such as IQL struggle perhaps due to a lack of shared state. MAPPO, despite struggling in the no energy team configurations achieves its best performance in the specialized setting with energy (PSE = 0.97), indicating that role specialization might mitigate coordination difficulty in this shared task setting. Surprisingly across both tasks as seen in Figure 4, agents tend to converge faster in the energy-constrained setting than in the no-energy baseline. This suggests that the structured turn-taking enforced by energy levels of agents in the shared task mode may simplify coordination rather than hinder performance, perhaps leading to more straightforward credit assignment and role specialization during learning.

6 Experiment 2: FairSkillMARL

6.1 Baseline Methods

We compare FairSkillMARL to two standard fairness methods across 500K timesteps and 4 seeds to investigate how well our framework performs in terms of skill-task alignment, workload, and both. **Gini Index** is a derivative of FairSkillMARL with $\alpha = 1$, thus, it measures agents’ contribution to sub-tasks in the reward function [54, 18]. **Fair Efficient Network (FEN)** measures agent resource utilization and penalizes agents when they deviate from the average utilization of all agents [55].



Figure 5: L_3 composite disparity over training timesteps for different algorithms and skill configurations with no energy. Lower values indicate fairer agent behavior.

6.2 Training and Testing Procedure

We conduct two controlled experiments across 500K timesteps and 4 seeds to isolate the effects of different fairness components. First, to isolate the impact of L_2 , we compared skill-task alignment ($\alpha = 0.7$) against workload only fairness ($\alpha = 0$) across four fairness weights ($\lambda \in \{5, 50, 100, 300\}$) using specialized teams due to their varying skill levels. Second, we compare all on-policy and off-policy MARL algorithms from Experiment 1 to evaluate fair task distributions in terms of workload and skill-alignment using the efficiency-based reward function, $R(s_t, \mathbf{a}_t)$. We used the specialised team setting with 3 agents for the rescue breaths task. All agents’ energy levels were set to 0; hence, the shared task mode was not explored.

6.3 Measures

In addition to **success rate**, we use Workload balance and Alignment score as performance metrics to assess agents ability to balance workload and skill-task alignment as they aim to reach the goal.

Alignment score measures the degree to which agents perform tasks aligned with their skill level, with 1.0 that indicates perfect alignment and 0 indicating random assignment. Specifically, it is the mean, over tasks executed in an episode, of the fraction performed by the task’s most-skilled agent (1 = perfect specialist use versus 0 = random). To the best of our knowledge, no prior MARL work quantifies fairness as the average fraction of tasks executed by the most-skilled agent; the alignment score is therefore a novel contribution of this paper. See supplementary for mathematical formulation.

Range Workload balance is evaluated via the *range* of normalized contributions, defined as the difference between the maximum and minimum agent contributions. The range is the extent of workload distribution across agents, with 0 corresponding to perfectly balanced task sharing, while 1 reveals disproportionate burden. Range is a standard measure of workload equity in scheduling and routing research [? ?]. Meanwhile, the normalised contributions are calculated via the Gini index, which measures average pairwise disparity in contributions normalized by the mean. Gini-based fairness metrics have been applied in MARL settings such as stock-trading [56] and traffic-signal control[57]. Combining these workload metrics with the alignment score provides a comprehensive assessment of fairness.

6.4 FairSkillMARL Results

6.4.1 Comparison to Workload only baselines (GINI and FEN)

We evaluate the effect of skill-task alignment (L_2) by comparing FairSkillMARL ($\alpha = 0.7$) performance with workload-only baselines (QMIX Gini, $\alpha = 1.0$ and FEN) across fairness weights $\lambda \in \{5, 50, 100, 300\}$. Our results from Table 3 show that across all conditions, FairSkillMARL achieves higher alignment scores while maintaining comparable or superior success rates. A higher alignment score indicates that agents more frequently perform tasks matching their specialized skills (better coordination), whereas a lower workload range reflects more balanced task sharing across the team.

Across fairness coefficients ($\lambda = 5-300$), *FairSkillMARL* ($\alpha = 0.7$) consistently outperforms workload-only baselines (*FEN* and *QMIX Gini*) in both coordination quality and fairness. At moderate fairness weights ($\lambda = 5, 50$), *FairSkillMARL* improves alignment by **40–60%** relative to *FEN* and by **15–25%** over *QMIX Gini*, while reducing workload range by roughly **50%** (0.06 vs. 0.10–0.18). At higher fairness levels ($\lambda = 100, 300$), *FairSkillMARL* achieves stronger specialization. Alignment scores are **40–600% higher** than *FEN* and **35–40% higher** than *QMIX Gini*, while workload range is reduced by **70–85%**. Despite the stronger regularization, success rates remain comparable or higher (0.80–0.83 vs. 0.40–0.86), indicating that incorporating explicit skill–task alignment (L_2) enables teams to remain both fair and efficient even under strong fairness constraints. We expect ($\alpha = 0.0$) to have the highest alignment score, as the fairness reward is collapsed to only the L_2 skill-task alignment metric after that. For ($\lambda = 5, 50, 100$), we observe that trend further confirming the impact of L_2 .

Table 3: Ablation study results to show the impact of skill-task alignment on specialized teams. Higher alignment and lower range indicate better coordination and fairness.

Method	λ	α	Success Rate \uparrow	Alignment Score \uparrow	Range \downarrow
FEN[17]		-	0.80 ± 0.02	0.32 ± 0.07	0.18 ± 0.09
QMIX Gini [18]	5	1.0	0.82 ± 0.06	0.33 ± 0.08	0.06 ± 0.01
QMIX FairSkillMARL (Ours)		0.0	0.80 ± 0.05	0.46 ± 0.19	0.07 ± 0.03
QMIX FairSkillMARL (Ours)		0.7	0.83 ± 0.04	0.32 ± 0.16	0.06 ± 0.01
FEN [17]		-	0.86 ± 0.10	0.29 ± 0.03	0.06 ± 0.00
QMIX Gini [18]	50	1.0	0.80 ± 0.03	0.42 ± 0.12	0.08 ± 0.05
QMIX FairSkillMARL (Ours)		0.0	0.82 ± 0.04	0.48 ± 0.13	0.10 ± 0.06
QMIX FairSkillMARL (Ours)		0.7	0.83 ± 0.05	0.46 ± 0.18	0.06 ± 0.01
FEN [17]		-	0.40 ± 0.06	0.08 ± 0.03	0.36 ± 0.02
QMIX Gini [18]	100	1.0	0.83 ± 0.04	0.40 ± 0.10	0.17 ± 0.07
QMIX FairSkillMARL (Ours)		0.0	0.80 ± 0.00	0.56 ± 0.00	0.05 ± 0.00
QMIX FairSkillMARL (Ours)		0.7	0.76 ± 0.00	0.22 ± 0.00	0.10 ± 0.00
FEN [17]		-	0.40 ± 0.06	0.10 ± 0.02	0.37 ± 0.01
QMIX Gini [17]	300	1.0	0.83 ± 0.00	0.23 ± 0.00	0.10 ± 0.00
QMIX FairSkillMARL (Ours)		0.0	0.82 ± 0.06	0.41 ± 0.11	0.05 ± 0.01
QMIX FairSkillMARL (Ours)		0.7	0.76 ± 0.00	0.55 ± 0.00	0.05 ± 0.00

These results demonstrate that including skill–task alignment (L_2) in the fairness definition produces fair teams with **better coordination**, unlike workload-only approaches, which focus on equalised efforts without considering agent specialization. **This robustness is most evident at extreme fairness ($\lambda = 300$), where FEN degrades to 40% success while FairSkillMARL maintains 76% success, showing that skill-aware coordination remains effective where pure workload balancing may fail.** Interestingly, in some settings ($\lambda = 5, 50, 100$), $\alpha = 0$ yields higher alignment and lower range because the fairness reward ($L_3 = \alpha L_1 + (1 - \alpha)L_2$) focuses solely on skill–task alignment, leading to more coordinated behavior and efficient completion of tasks. Meanwhile, higher α (e.g., 0.7) prioritizes workload balance at the cost of specialization.

6.4.2 Comparison Across Algorithms

We investigated the emergent fairness of standard MARL algorithms without fairness reward shaping. IQL and VDN exhibit severe agent imbalance, while MAPPO achieves balanced coordination. Under energy constraints, MAPPO remains robust, and value-based methods (IQL, VDN, QMIX) continue to show imbalance as seen in Figure 5.

7 Experiment 3: FairSkillMARL Ablation

7.1 Baseline Methods, Training, and Testing Procedure

We compared FairSkillMARL variants from Experiment 6.1 against workload baselines (FEN and QMIX Gini) at moderate fairness parameter $\lambda = 50$ across 500k timesteps with 6 seeds. Our specialised team setting here has all agents’ energy levels set to 0, hence the shared task mode was not explored.

7.2 Measures

Our experimental design involves three independent variables (Algorithm type, fairness penalty magnitude (λ), and random seeds. Primary dependent variables were success rate and skill-task alignment score. We use Mann-Whitney U tests, a non-parametric method robust to non-normal distributions common in RL experiments.

7.3 Statistical Significance Results

When configured to prioritize skill-task alignment ($\alpha=0.0$), FairSkillMARL achieves marginally significantly higher alignment scores than FEN (0.48 vs 0.29, $p=0.095$, effect size $r=0.47$), implying that imposing the skill-task fairness penalty can improve agent’s skill alignment to their tasks. At $\alpha = 1.0$, FairSkillMARL behaves similarly to QMIX Gini, showing that our framework includes existing fairness methods as a special case. This demonstrates that our α parameter correctly controls the fairness objective.

8 Conclusion

In this work, we introduced skill-task alignment as a fairness criterion for heterogeneous agents in MARL. We also introduced MARLHospital, a customizable simulation environment for benchmarking cooperative MARL algorithms on varying skill levels and energy levels across task difficulty levels. We evaluated four standard MARL algorithms across two tasks with three agents with different skill levels and energy cost constraints. We found that CTDE algorithms achieved the best performance in both the CPR task and the rescue breaths tasks. Also, our experiments show that FairSkillMARL achieves a statistically significant improvement at $\alpha=0.7$ compared to the FEN algorithm, and that our approach captures skill misalignment in complex coordination tasks. By modeling agent capabilities explicitly, our method provides a foundation for fairness definitions that consider both workload and agent skills in heterogeneous teams. Future research can build upon this foundation to explore multi-objective optimization techniques, and applications to larger-scale heterogeneous multi-agent systems.

References

- [1] Angelique Taylor, Tauhid Tanjim, Michael Joseph Sack, Maia Hirsch, Kexin Cheng, Kevin Ching, Jonathan St George, Thijs Roumen, Malte F. Jung, and Hee Rin Lee. Rapidly Built Medical Crash Cart! Lessons Learned and Impacts on High-Stakes Team Collaboration in the Emergency Room, February 2025. arXiv:2502.18688 [cs] version: 1.
- [2] Angelique Taylor, Tauhid Tanjim, Huajie Cao, and Hee Rin Lee. Towards Collaborative Crash Cart Robots that Support Clinical Teamwork. In *Proceedings of the 2024 ACM/IEEE International Conference on Human-Robot Interaction, HRI '24*, pages 715–724, New York, NY, USA, March 2024. Association for Computing Machinery.
- [3] Angelique Taylor, Hee Rin Lee, Alyssa Kubota, and Laurel D. Riek. Coordinating Clinical Teams: Using Robots to Empower Nurses to Stop the Line. *Proceedings of the ACM on Human-Computer Interaction*, 3(CSCW):1–30, November 2019.
- [4] Ardi Tampuu, Tabet Matiisen, Dorian Kodolja, Ilya Kuzovkin, Kristjan Korjus, Juhan Aru, Jaan Aru, and Raul Vicente. Multiagent Cooperation and Competition with Deep Reinforcement Learning, November 2015.
- [5] Christian Schroeder de Witt, Tarun Gupta, Denys Makoviichuk, Viktor Makoviyuchuk, Philip H. S. Torr, Mingfei Sun, and Shimon Whiteson. Is Independent Learning All You Need in the StarCraft Multi-Agent Challenge?, November 2020.
- [6] Peter Sunehag, Guy Lever, Audrunas Gruslys, Wojciech Marian Czarnecki, Vinicius Zambaldi, Max Jaderberg, Marc Lanctot, Nicolas Sonnerat, Joel Z. Leibo, Karl Tuyls, and Thore Graepel. Value-Decomposition Networks For Cooperative Multi-Agent Learning, June 2017.
- [7] Tabish Rashid, Mikayel Samvelyan, Christian Schroeder de Witt, Gregory Farquhar, Jakob Foerster, and Shimon Whiteson. QMIX: Monotonic Value Function Factorisation for Deep Multi-Agent Reinforcement Learning, June 2018.
- [8] Micah Carroll, Rohin Shah, Mark K. Ho, Thomas L. Griffiths, Sanjit A. Seshia, Pieter Abbeel, and Anca Dragan. On the Utility of Learning about Humans for Human-AI Coordination, January 2020.
- [9] Huaxiaoyue Wang, Gonzalo Gonzalez-Pumariega, Yash Sharma, and Sanjiban Choudhury. Demo2Code: From Summarizing Demonstrations to Synthesizing Code via Extended Chain-of-Thought, November 2023.
- [10] Mikayel Samvelyan, Tabish Rashid, Christian Schroeder de Witt, Gregory Farquhar, Nantas Nardelli, Tim G. J. Rudner, Chia-Man Hung, Philip H. S. Torr, Jakob Foerster, and Shimon Whiteson. The StarCraft Multi-Agent Challenge, December 2019.
- [11] Benjamin Ellis, Jonathan Cook, Skander Moalla, Mikayel Samvelyan, Mingfei Sun, Anuj Mahajan, Jakob N. Foerster, and Shimon Whiteson. SMACv2: An Improved Benchmark for Cooperative Multi-Agent Reinforcement Learning, October 2023.
- [12] Edward Hughes, Joel Z. Leibo, Matthew G. Phillips, Karl Tuyls, Edgar A. Duéñez-Guzmán, Antonio García Castañeda, Iain Dunning, Tina Zhu, Kevin R. McKee, Raphael Koster, Heather Roff, and Thore Graepel. Inequity aversion improves cooperation in intertemporal social dilemmas, September 2018. arXiv:1803.08884 [cs].
- [13] Mingqi Yuan, Qi Cao, Man-On Pun, and Yi Chen. Multi-Agent Reinforcement Learning-Based Fairness-Aware Scheduling for Bursty Traffic. In *2021 IEEE Global Communications Conference (GLOBECOM)*, pages 1–6, December 2021.
- [14] Wanqing Fang, Xintian Zhao, and Chengwei Zhang. Fairness-aware multi-agent reinforcement learning and visual perception for adaptive traffic signal control. *Optoelectronics Letters*, 20(12):764–768, December 2024.

- [15] Xingshuai Huang, Di Wu, and Benoit Boulet. Fairness-Aware Model-Based Multi-Agent Reinforcement Learning for Traffic Signal Control. September 2022.
- [16] Jasmine Jerry Aloor, Siddharth Nayak, Sydney Dolan, and Hamsa Balakrishnan. Cooperation and Fairness in Multi-Agent Reinforcement Learning, October 2024.
- [17] Jiechuan Jiang and Zongqing Lu. Learning Fairness in Multi-Agent Systems, October 2019. arXiv:1910.14472 [cs].
- [18] Gabriele La Malfa, Jie M. Zhang, Michael Luck, and Elizabeth Black. Fairness Aware Reinforcement Learning via Proximal Policy Optimization, September 2025. arXiv:2502.03953 [cs].
- [19] Junkai Li, Siyu Wang, Meng Zhang, Weitao Li, Yunghwei Lai, Xinhui Kang, Weizhi Ma, and Yang Liu. Agent Hospital: A Simulacrum of Hospital with Evolvable Medical Agents, May 2024.
- [20] Paul Maria Scheickl, Balázs Gyenes, Tornike Davitashvili, Rayan Younis, André Schulze, Beat P. Müller-Stich, Gerhard Neumann, Martin Wagner, and Franziska Mathis-Ullrich. Cooperative Assistance in Robotic Surgery through Multi-Agent Reinforcement Learning. In *2021 IEEE/RSJ International Conference on Intelligent Robots and Systems (IROS)*, pages 1859–1864, September 2021. arXiv:2110.04857 [cs].
- [21] Xinzhi Zhang, Yeming Yang, Qingling Zhu, Qiuzhen Lin, Weineng Chen, Jianqiang Li, and Carlos A. Coello Coello. Multi-agent deep Q-network-based metaheuristic algorithm for Nurse Rostering Problem. *Swarm and Evolutionary Computation*, 87:101547, June 2024.
- [22] Ran Gong, Qiuyuan Huang, Xiaojian Ma, Hoi Vo, Zane Durante, Yusuke Noda, Zilong Zheng, Song-Chun Zhu, Demetri Terzopoulos, Li Fei-Fei, and Jianfeng Gao. MindAgent: Emergent Gaming Interaction, September 2023.
- [23] Xavier Puig, Kevin Ra, Marko Boben, Jiaman Li, Tingwu Wang, Sanja Fidler, and Antonio Torralba. VirtualHome: Simulating Household Activities via Programs, June 2018.
- [24] Cinjon Resnick, Wes Eldridge, David Ha, Denny Britz, Jakob Foerster, Julian Togelius, Kyunghyun Cho, and Joan Bruna. Pommerman: A Multi-Agent Playground, September 2018. Publication Title: arXiv.org.
- [25] John P. Agapiou, Alexander Sasha Vezhnevets, Edgar A. Duéñez-Guzmán, Jayd Matyas, Yiran Mao, Peter Sunehag, Raphael Köster, Udari Madhushani, Kavya Koppurapu, Ramona Comanescu, D. J. Strouse, Michael B. Johanson, Sukhdeep Singh, Julia Haas, Igor Mordatch, Dean Mobbs, and Joel Z. Leibo. Melting Pot 2.0, October 2023.
- [26] Qian Yue Hao, Fengli Xu, Lin Chen, Pan Hui, and Yong Li. Hierarchical Multi-agent Model for Reinforced Medical Resource Allocation with Imperfect Information. *ACM Transactions on Intelligent Systems and Technology*, 14(1):1–27, February 2023.
- [27] Dario Esposito, Davide Schaumann, Domenico Camarda, and Yehuda E. Kalay. Multi-Agent Modelling and Simulation of Hospital Acquired Infection Propagation Dynamics by Contact Transmission in Hospital Wards. In Yves Demazeau, Tom Holvoet, Juan M. Corchado, and Stefania Costantini, editors, *Advances in Practical Applications of Agents, Multi-Agent Systems, and Trustworthiness. The PAAMS Collection*, pages 118–133, Cham, 2020. Springer International Publishing.
- [28] Xueting Luo, Hao Deng, Jihong Yang, Yao Shen, Huanhuan Guo, Zhiyuan Sun, Mingqing Liu, Jiming Wei, and Shengjie Zhao. H2-MARL: Multi-Agent Reinforcement Learning for Pareto Optimality in Hospital Capacity Strain and Human Mobility during Epidemic, March 2025.
- [29] Harsha Koduri. NurseSchedRL: Attention-Guided Reinforcement Learning for Nurse-Patient Assignment, September 2025. arXiv:2509.18125 [cs].
- [30] Jose M. Ruiz Mejia and Danda B. Rawat. MedScrubCrew: A Medical Multi-Agent Framework for Automating Appointment Scheduling Based on Patient-Provider Profile Resource Matching. *Healthcare*, 13(14):1649, July 2025. Publisher: Multidisciplinary Digital Publishing Institute.
- [31] Angélica Torres-Huesca, Luis-Gerardo Montané-Jiménez, and María-Teresa Cepero-García. MULTI-AGENT COLLABORATIVE WORK SIMULATION FOR PATIENT CARE IN HOSPITALS. *DYNA New Technologies Journal*, 8(1), 2021.
- [32] Christopher Amato. A First Introduction to Cooperative Multi-Agent Reinforcement Learning, December 2024.
- [33] John Schulman, Filip Wolski, Prafulla Dhariwal, Alec Radford, and Oleg Klimov. Proximal Policy Optimization Algorithms, August 2017.
- [34] Chao Yu, Akash Velu, Eugene Vinitzky, Jiaxuan Gao, Yu Wang, Alexandre Bayen, and Yi Wu. The Surprising Effectiveness of PPO in Cooperative, Multi-Agent Games, November 2022.
- [35] Jakob Foerster, Gregory Farquhar, Triantafyllos Afouras, Nantas Nardelli, and Shimon Whiteson. Counterfactual Multi-Agent Policy Gradients. *Proceedings of the AAAI Conference on Artificial Intelligence*, 32(1), April 2018.

- [36] Dilruk Perera, Siqi Liu, and Mengling Feng. Demystifying Complex Treatment Recommendations: A Hierarchical Cooperative Multi-Agent RL Approach. In *2023 International Joint Conference on Neural Networks (IJCNN)*, pages 1–10, June 2023.
- [37] Daniel J. Tan, Qianyi Xu, Kay Choong See, Dilruk Perera, and Mengling Feng. Advancing Multi-Organ Disease Care: A Hierarchical Multi-Agent Reinforcement Learning Framework, September 2024.
- [38] William H. Guss, Brandon Houghton, Nicholay Topin, Phillip Wang, Cayden Codel, Manuela Veloso, and Ruslan Salakhutdinov. MineRL: A Large-Scale Dataset of Minecraft Demonstrations, July 2019.
- [39] Gonzalo Gonzalez-Pumariiega, Leong Su Yean, Neha Sunkara, and Sanjiban Choudhury. Robotouille: An Asynchronous Planning Benchmark for LLM Agents, February 2025. arXiv:2502.05227 [cs].
- [40] Robert Bredereck. Computing Efficient Envy-Free Partial Allocations of Indivisible Goods. 2025.
- [41] Siddharth Barman, Debajyoti Kar, and Shraddha Pathak. Parameterized Guarantees for Almost Envy-Free Allocations. *New Zealand*, 2024.
- [42] Dolev Mutzari. Resilient Fair Allocation of Indivisible Goods. 2023.
- [43] Jonathan Scarlett. For One and All: Individual and Group Fairness in the Allocation of Indivisible Goods. 2023.
- [44] Jacobus Smit. Fairness and Cooperation between Independent Reinforcement Learners through Indirect Reciprocity. *New Zealand*, 2024.
- [45] Archit Sood. Fairness of Exposure in Online Restless Multi-armed Bandits. *New Zealand*, 2024.
- [46] Umer Siddique. Towards Fair and Efficient Policy Learning in Cooperative Multi-Agent Reinforcement Learning. 2025.
- [47] Georgios Papoudakis, Filippos Christianos, Lukas Schäfer, and Stefano V. Albrecht. Benchmarking Multi-Agent Deep Reinforcement Learning Algorithms in Cooperative Tasks, November 2021.
- [48] Frans Oliehoek and Christopher Amato. A Concise Introduction to Decentralized POMDPs. January 2016.
- [49] Soravit Savatmongkornkul, Chaiyaporn Yuksen, Sumalin Chumkot, Pongsakorn Atiksawedparit, Chetsadakon Jenpanitpong, Sorawich Watcharakitpaisan, Parama Kaninworapan, and Konwachira Maijan. Comparison of chest compression quality between 2-minute... : International Journal of Critical Illness and Injury Science.
- [50] Jakob Foerster, Ioannis Alexandros Assael, Nando de Freitas, and Shimon Whiteson. Learning to Communicate with Deep Multi-Agent Reinforcement Learning. In *Advances in Neural Information Processing Systems*, volume 29. Curran Associates, Inc., 2016.
- [51] He He, Jordan Boyd-Graber, Kevin Kwok, and Hal Daumé III. Opponent Modeling in Deep Reinforcement Learning, September 2016.
- [52] Yali Du, Lei Han, Meng Fang, Ji Liu, Tianhong Dai, and Dacheng Tao. LIIR: Learning Individual Intrinsic Reward in Multi-Agent Reinforcement Learning. In *Advances in Neural Information Processing Systems*, volume 32. Curran Associates, Inc., 2019.
- [53] Volodymyr Mnih, Koray Kavukcuoglu, David Silver, Alex Graves, Ioannis Antonoglou, Daan Wierstra, and Martin Riedmiller. Playing Atari with Deep Reinforcement Learning, December 2013.
- [54] Robert Busa-Fekete, Balazs Szorenyi, Paul Weng, and Shie Mannor. Multi-objective Bandits: Optimizing the Generalized Gini Index, June 2017. arXiv:1706.04933 [cs].
- [55] Jiechuan Jiang and Zongqing Lu. Learning Fairness in Multi-Agent Systems, October 2019. arXiv:1910.14472 [cs].
- [56] Fairness in Multi-agent Reinforcement Learning for Stock Trading.
- [57] Umer Siddique, Peilang Li, and Yongcan Cao. Fairness in Traffic Control: Decentralized Multi-agent Reinforcement Learning with Generalized Gini Welfare Functions.
- [58] Volodymyr Mnih, Koray Kavukcuoglu, David Silver, Andrei A. Rusu, Joel Veness, Marc G. Bellemare, Alex Graves, Martin Riedmiller, Andreas K. Fidjeland, Georg Ostrovski, Stig Petersen, Charles Beattie, Amir Sadik, Ioannis Antonoglou, Helen King, Dharshan Kumaran, Daan Wierstra, Shane Legg, and Demis Hassabis. Human-level control through deep reinforcement learning. *Nature*, 518(7540):529–533, February 2015.

A MARLHospital Environment

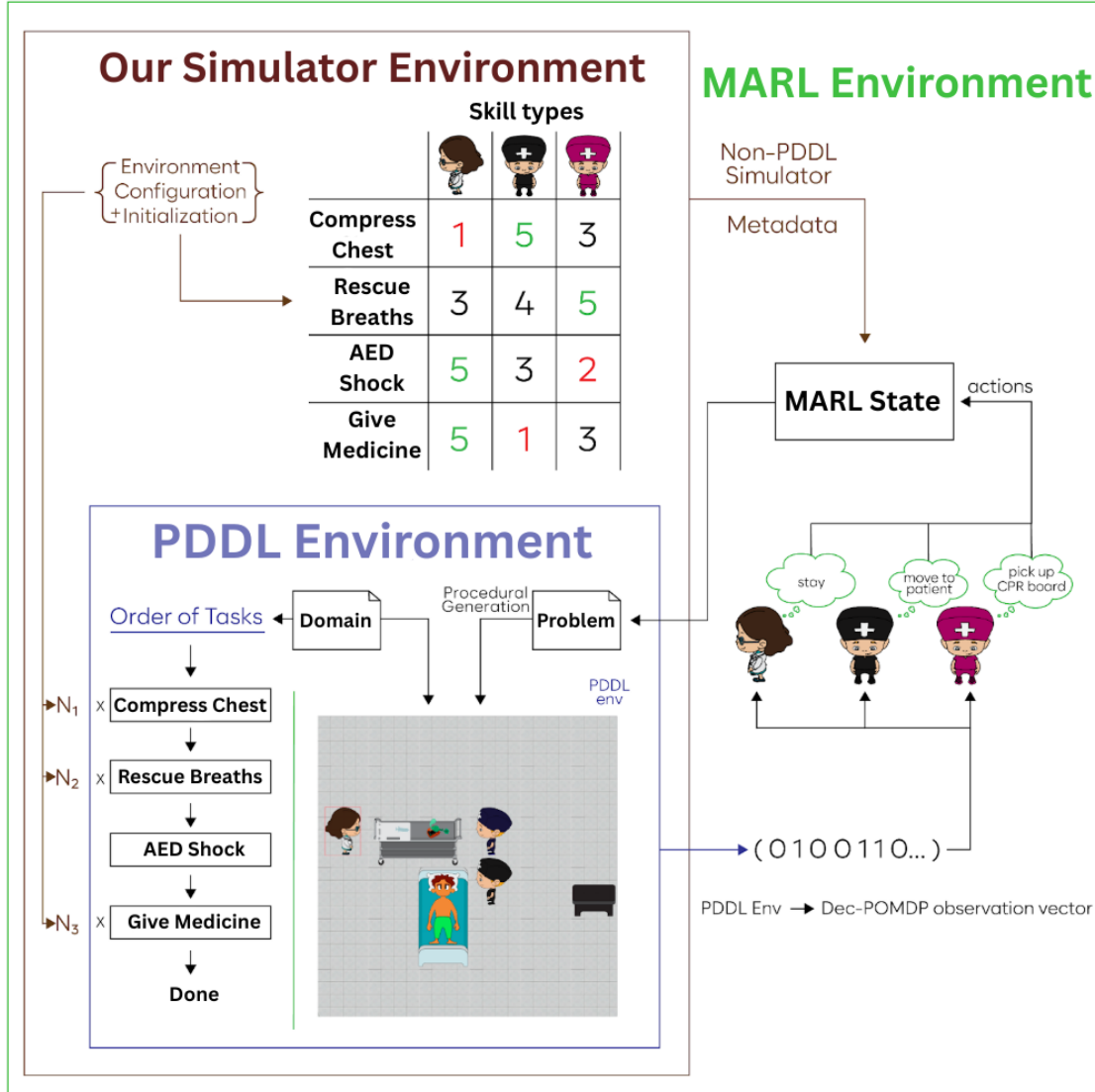


Figure 6: MARLHospital environment: Breakdown of the PDDL environment wrapped by the MARL environment with 3 HCW agents and a patient.

Figure 6 shows how the Planning Domain Definition Language (PDDL) and MARL environment are integrated within MARLHospital in the baseline configuration. A configuration file initializes 1) the agent, station, patient, and object positions in the PDDL environment, 2) the skill (and possibly initial energy) levels of the agents, and 3) the subtask requirements to reach the goal. In the default setting, agents receive a binary encoding of the PDDL environment as an observation; when skill information is included in the observation, that data is passed from the configuration as well. The MARL state converts agents' actions into pddl actions based on state factors such as skill level, energy, and subtask requirements marked by N_1 , N_2 , and N_3 in the diagram.

The remainder of this section provides an overview of the different components of the PDDL environment.

Players consist of the healthcare workers in the environment. Controlled by the RL agents, they take actions in the PDDL environment, and are allowed to move to locations on the grid adjacent to stations. See Figure 7 for player options.

Actions consist of the actions healthcare workers can perform within the environment. These include the following:



Figure 7: The PDDL players, controlled by RL agents

- Move: move the worker from station A to station B
- Pick-up: pick up an item at the worker’s current station. Afterwards, the station is empty and the worker now holds the item.
- Place: place the item the worker is holding on the worker’s current station. Before placing an item, the station must be empty. Afterwards player no longer holds an item.
- Unstack: unstack the item that is on top of another item at the worker’s current station. The unstacked item is now held by the worker.
- Stack: stack an item on top of another item at the worker’s current station. The worker no longer holds an item.
- Stack under: stack an item underneath another item at the worker’s current station.
- Chest compression: perform a medical procedure in which the worker manually circulates the blood of the patient. Before compressing chest, the patient must have a CPR board underneath them.
- Rescue breaths: perform a medical procedure in which the worker directly provides oxygen to the patient. Before giving rescue breaths, the patient must have a breathing pump attached.
- Give shock: perform a medical a medical procedure in which the worker uses a defibrillator to restart the patient’s heart. The patient must have an AED device connected to them.
- Give medicine: perform a medical procedure in which the worker administers medicine to the patient through a syringe. The syringe must be on the patient.

moving between stations, picking up or placing items, stacking or unstacking objects (including stacking under), and performing medical procedures such as chest compressions and rescue breaths.

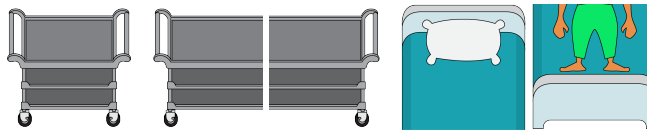


Figure 8: PDDL stations.

Stations are a class of immovable objects in the environment. Players can move to unoccupied cells adjacent to stations, as mentioned earlier, and items can be placed on stations. See available station assets in Figure 8.



Figure 9: Item assets. *Left*: Items used for treatment. From left to right: syringe, CPR board, breathing pump, AED device. *Right*: Patient in various states. From left to right: default, after chest compressions, after rescue breaths, after AED shock, after given medicine

Items are interactable objects in the environment. Apart from the patient, the items in MARLHospital are tools necessary for the HCWs to complete tasks in treating the patient. They can be picked up and placed down by Players on stations. Items can be stacked on top of one another, though the player can only pick up the item at the top of a stack. To perform treatment actions, certain items need to be stacked on the patient based on that treatment action: a CPR board for `compress_chest`, a breathing pump for `give_rescue_breaths`, an AED device for `giving_shock`, and a syringe for `giving_medicine`.

There are two items with special properties in the environment. The first is the CPR board, which, unlike other items, can also be stacked under the patient. The second is the patient itself. Unlike other items, the patient cannot be moved

from the patient bed station, and it is the only possible predicate of treatment actions. The patient is rendered with different states based on the most recent task completed on them. See Figure 9 for item and patient assets.

Observation Space Size. The observation space consists of a total of 174 boolean values. Each of the three agents receives an individual observation vector of size 58. These 58 boolean features are structured as follows:

- **Patient State (4 booleans):** Indicates whether the patient has been chest compressed, rescue breathed, treated, or shocked.
- **Agent Locations (18 booleans):** Encodes the location of each of the three agents, where each agent can be at one of six discrete stations: `hospital_cart_right1`, `table1`, `hospital_cart1`, `hospital_cart_left1`, `patient_legs1`, or `patient_bed_station1`.
- **Held Items (9 booleans):** Indicates which item (if any) is held by each of the three agents. Possible items include: `pump1`, `cpr_board1`, and `patient1`.
- **Skill Levels (18 booleans):** Represents each agent’s skill level (unskilled, beginner, expert) for two skills: chest compression and rescue breathing.
- **Available Actions (9 booleans):** Encodes which actions are currently available to the agent, such as treating the patient, moving to any of the six stations, moving an item, or stacking an item under another.

B MARLHospital Environment

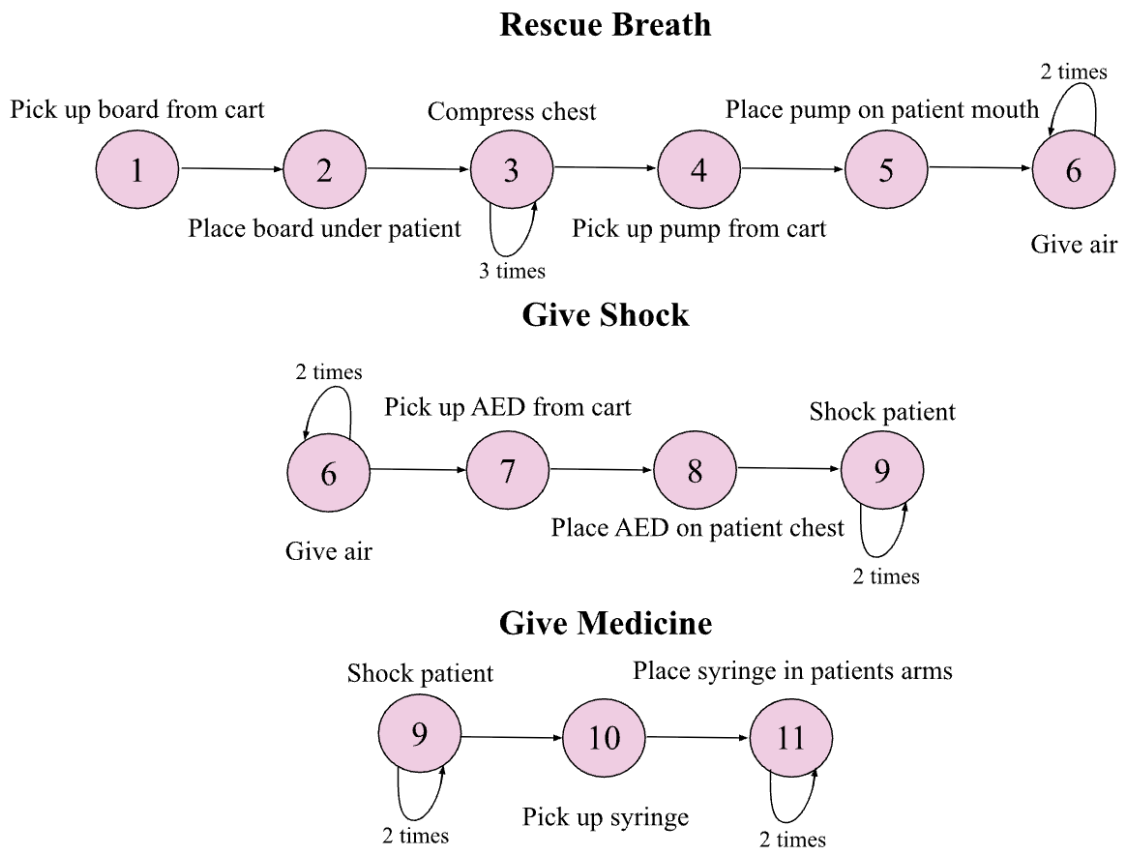


Figure 10: MARLHospital environment: Breakdown of the PDDL environment wrapped by the MARL environment with 3 HCW agents and a patient.

Table 4: Comparison between MARLHospital and other simulators

	Multi-Agent	MARL	Hospital Setting	Skill Specialization	Variable Skills	Energy Levels	Fairness Support
Overcooked-AI [8]	✓	✗	✗	✗	✗	✗	✗
Agent Hospital [19]	✓	✗	✓	✓ ¹	✗	✗	✗
MARL Robotic Surgery [?]	✓	✓	✓ ²	✓	✗	✗	✗
MARL for Nurse Rostering [21]	✓	✓	✓ ³	✗	✗	✗	✗
Cuisine World [22]	✓	✗	✗	✗	✗	✗	✗
VirtualHome [23]	✓	✗	✗	✗	✗	✗	✗
SMACv2 [11]	✓	✓	✗	✓	✗	✗	✗
Pommerman [24]	✓	✓	✗	✗	✗	✗	✗
Melting Pot 2.0 [25]	✓	✓	✗	✓	✗	✗	✗
Robotouille [39]	✓	✗	✗	✗	✗	✓	✗
HMARL for Medical Allocation [26]	✓	✓	✗	✗	✗	✗	✗
MA Hospital Infection Sim [27]	✓	✗	✓	✓	✗	✗	✗
<i>MARLHospital</i>	✓	✓	✓	✓	✓	✓	✓

C Selected Hyperparameters

For hyperparameter tuning in MARLHospital, we primarily conducted a grid search and did a sweep across several hyperparameters for all the algorithms, ensuring consistency with established MARL benchmarks. The hyperparameter selection process follows a structured approach that is compatible with prior algorithms’ work.

The hyperparameters for each algorithm, including IQL, MAPPO, VDN, and QMIX, are outlined in Tables 5 to 8. Key parameters include the hidden dimension size, learning rate, reward standardization, network type (e.g., GRU or fully connected networks), target update frequency, entropy coefficient (for policy gradient methods), and the number of steps used in bootstrapping (n-step returns).

For off-policy algorithms such as IQL, VDN, and QMIX, an experience replay buffer is employed to decorrelate samples and stabilize learning, following standard practices [58]. On-policy algorithms like MAPPO utilises parallel synchronous workers to mitigate sample correlation and improve stability during training.

The hyperparameter configurations for the IQL algorithm, with parameter sharing for MARLHospital is shown in Table 5.

Table 5: Hyperparameters for IQL with parameter sharing.

MARLHospital	
hidden dimension	64
learning rate	0.0005
reward standardisation	False
network type	GRU
evaluation epsilon	0.0
target update	20 (hard)

“The ‘target update 0.01 (soft)’ in our MAPPO implementations is based on Polyak averaging, where the target critic network is updated slowly using 1% new and 99 old weights for stability. Although we did not add it to the hyperparameter table, the PPO clipping coefficient is set to 0.2 and is used to constrain policy updates during training.

The hyperparameter configurations for the MAPPO algorithm, with parameter sharing for MARLHospital is shown in Table 6.

The hyperparameter configurations for the VDN algorithm, with parameter sharing for MARLHospital is shown in Table 7.

The hyperparameter configurations for the QMIX algorithm, with parameter sharing for MARLHospital, are shown in Table 8.

Table 6: Hyperparameters for MAPPO with parameter sharing.

MARLHospital	
hidden dimension	64
learning rate	0.002
reward standardisation	True
network type	GRU
entropy coefficient	0.01
target update	0.05 (soft)
clipping coef	0.2

Table 7: Hyperparameters for VDN with parameter sharing.

MARLHospital	
hidden dimension	64
learning rate	0.001
reward standardisation	False
network type	GRU
evaluation epsilon	0.0
target update	25 (hard)

Table 8: Hyperparameters for QMIX with parameter sharing.

MARLHospital	
hidden dimension	64
learning rate	0.001
reward standardisation	False
network type	GRU
evaluation epsilon	0.1
target update	25 (hard)

```

"config": {
  "num_compressions": {
    "patient": 3,
    "default": 3
  },
  "num_breaths": {
    "patient": 2,
    "default": 2
  },
  "num_shocks": {
    "patient": 2,
    "default": 2
  },
  "num_medicine_doses": {
    "patient": 2,
    "default": 2
  },
  "energy_levels": {
    "compresschest_cost": 0,
    "recharge_rate": 100,
    "max": 1000
  },
  "num_players": 3
}

```

Figure 11: JSON to configure the necessary steps to treat the patient

```

{
  "name": "robot",
  "x": 0,
  "y": 3,
  "direction": [
    1,
    0
  ],
  "actions": [
    "move",
    "moveitem",
    "compresschest",
    "giverescuebreaths",
    "giveshock",
    "givemedicine"
  ],
  "skill_info": {
    "compresschest": 1,
    "giverescuebreaths": 1,
    "giveshock": 1,
    "givemedicine": 1
  }
},

{
  "name": "robot",
  "x": 3,
  "y": 3,
  "direction": [
    -1,
    0
  ],
  "actions": [
    "move",
    "moveitem",
    "compresschest",
    "giverescuebreaths",
    "giveshock",
    "givemedicine"
  ],
  "skill_info": {
    "compresschest": 1,
    "giverescuebreaths": 1,
    "giveshock": 1,
    "givemedicine": 1
  }
},

{
  "name": "robot",
  "x": 4,
  "y": 3,
  "direction": [
    1,
    0
  ],
  "actions": [
    "move",
    "moveitem",
    "compresschest",
    "giverescuebreaths",
    "giveshock",
    "givemedicine"
  ],
  "skill_info": {
    "compresschest": 1,
    "giverescuebreaths": 1,
    "giveshock": 1,
    "givemedicine": 1
  }
}

```

Figure 12: JSON to configure the HCWs skill information for equal skill.

```

{
  "name": "robot",
  "x": 0,
  "y": 3,
  "direction": [
    1,
    0
  ],
  "actions": [
    "move",
    "moveitem",
    "compresschest",
    "giverescuebreaths",
    "giveshock",
    "givemedicine"
  ],
  "skill_info": {
    "compresschest": 3,
    "giverescuebreaths": 1,
    "giveshock": 1,
    "givemedicine": 1
  }
},

{
  "name": "robot",
  "x": 3,
  "y": 3,
  "direction": [
    -1,
    0
  ],
  "actions": [
    "move",
    "moveitem",
    "compresschest",
    "giverescuebreaths",
    "giveshock",
    "givemedicine"
  ],
  "skill_info": {
    "compresschest": 1,
    "giverescuebreaths": 2,
    "giveshock": 1,
    "givemedicine": 1
  }
},

{
  "name": "robot",
  "x": 4,
  "y": 3,
  "direction": [
    1,
    0
  ],
  "actions": [
    "move",
    "moveitem",
    "giverescuebreaths",
    "giveshock",
    "givemedicine"
  ],
  "skill_info": {
    "compresschest": 1,
    "giverescuebreaths": 1,
    "giveshock": 2,
    "givemedicine": 1
  }
}

```

Figure 13: JSON to configure the HCWs skill information for specialized roles.

```

{
  "name": "robot",
  "x": 0,
  "y": 3,
  "direction": [
    1,
    0
  ],
  "actions": [
    "move",
    "moveitem",
    "compresschest",
    "giverescuebreaths",
    "giveshock",
    "givemedicine"
  ],
  "skill_info": {
    "compresschest": 3,
    "giverescuebreaths": 0,
    "giveshock": 0,
    "givemedicine": 1
  }
},

{
  "name": "robot",
  "x": 3,
  "y": 3,
  "direction": [
    -1,
    0
  ],
  "actions": [
    "move",
    "moveitem",
    "compresschest",
    "giverescuebreaths",
    "giveshock",
    "givemedicine"
  ],
  "skill_info": {
    "compresschest": 0,
    "giverescuebreaths": 2,
    "giveshock": 0,
    "givemedicine": 1
  }
},

{
  "name": "robot",
  "x": 4,
  "y": 3,
  "direction": [
    1,
    0
  ],
  "actions": [
    "move",
    "moveitem",
    "compresschest",
    "giverescuebreaths",
    "giveshock",
    "givemedicine"
  ],
  "skill_info": {
    "compresschest": 0,
    "giverescuebreaths": 0,
    "giveshock": 2,
    "givemedicine": 1
  }
}

```

Figure 14: JSON to configure the HCWs skill information for required cooperation